

# Forming Evolution of Titanium Grade2 Sheets

**Merve Tekin**

Bursa Uludag Universitesi

**Rukiye Ertan** (✉ [rukiye@uludag.edu.tr](mailto:rukiye@uludag.edu.tr))

Bursa Uludag Universitesi <https://orcid.org/0000-0002-9631-4607>

**Hande Güler Özgül**

Bursa Uludag Universitesi

---

## Research Article

**Keywords:** Titanium, Hot forming, Springback, Mechanical properties, Microstructure

**Posted Date:** June 28th, 2021

**DOI:** <https://doi.org/10.21203/rs.3.rs-616163/v1>

**License:**  This work is licensed under a Creative Commons Attribution 4.0 International License.

[Read Full License](#)

---

**Version of Record:** A version of this preprint was published at Materials Testing on January 1st, 2022. See the published version at <https://doi.org/10.1515/mt-2021-2004>.

# Abstract

Titanium and its alloys take attention, especially in aerospace, automotive, and biomedical applications because of their strength, corrosion resistance biocompatibility. Titanium components, in general, are produced by sheet metal forming. However, the springback effect is a critical problem in the forming process due to the difficult formability of titanium sheets. In the present study, the hot forming process was applied to sheets to investigate the effect of deformation temperature on microstructure, mechanical properties, and springback behavior of commercially pure grade 2 (CP2) titanium sheets. The springback angles were measured at the CAD model after the sheets were scanned by the 3D scanner. The tensile test, hardness measurements, and microstructural analysis were examined by using specimens that were cut from the side-wall and bottom of the deformed sheet as U-profile. The results reveal that the microstructure is substantially changed, and springback is reduced with increasing temperature, and thus, optimum results were obtained compared to the data obtained at room temperature.

## 1. Introduction

The development of titanium alloys was started with aerospace applications because of the requirement of higher strength-to-weight ratios, stable mechanical properties at high temperatures, low density, and high corrosion resistance [1]. Because of these properties, titanium alloys were found in a more extensive range of application areas such as chemical, biomedical, marine, automotive, sports equipment, petroleum refining pulp, paper plants, etc. [2-4]. The titanium alloys have four groups,  $\alpha$  and near- $\alpha$  alloys, which are named commercially pure (CP) titanium as well,  $\beta$  alloys and  $\alpha+\beta$  alloys [5]. The commercially pure titanium is also divided into four classes which are from Grade 1 to 4. This classification is based on the carbon, oxygen, hydrogen, iron, and nitrogen content of titanium [1], and the yield strength increases from 170 MPa to 480 MPa, as the grade number increases [6].

Titanium alloys can be produced in various forms such as ingot, bar, billet, plate, strip, tube or sheet [7]. To form sheet metal titanium alloys, there are many forming processes, for example, roll forming, stretch forming, power spinning or press forming [8]. The cold press forming of titanium materials is difficult due to springback, and like other sheet materials, springback is a critical problem for the cold press forming process of titanium sheets [9].

Springback is occurred due to elastic recovery after removed the loading. The parameters such as sheet thickness, tool dimensions, contact between tool and workpiece, material properties have affected the magnitude of the springback [10,11]. Many researchers have investigated the springback behavior of titanium alloys and effective parameters. Ozturk et al. [12] studied the effect of temperature on the springback behavior of CP2 titanium sheets with a thickness of 0.8 mm. They aimed to found optimal forming parameters for CP2 titanium sheets and decrease the springback effect. Gisario et al. [13] achieved a higher bending angle and ignored the springback angle of CP2 titanium alloy with a combination of external force laser-assisted bending and contact pressure of the tool. Zhao et al. [14] investigated the influence of the electric pulse on the springback of Ti-6Al-4V. They found that

electric pulses can replace the conventional forming processes and effectively decrease the springback effect. Hamedon et al. [15] achieved that decrease forming load and increase the formability of Ti6Al4V titanium alloy by using resistance heating. Khayatzadeh et al. [16] investigated the factors that affect springback during the Gr50 titanium sheet alloy forming process. Li et al. [17] studied the springback behavior of high-strength titanium bent tubes and developed explicit/implicit 3D finite element models to correlate the springback with material properties and the geometrical dimensions. Another model was developed by Badr et al. [18]. They examined V-bending and roll forming for the mill annealed cold-rolled Ti-6Al-4V sheet and then developed FEA (Finite Element Analysis) simulation and HAH (Homogeneous Anisotropic Hardening) model. Ao et al. [19] examined the effect of electropulsing on springback and microstructure during V-bending of Ti-6Al-4V sheet. Gheysarian and Abbasi [20] applied solution treatment, annealing, and aging to Ti-6Al-4V titanium alloy sheets. Then, they studied the effect of aging on springback behavior and formability of Ti-6Al-4V.

In this study, a hot forming process was applied to increase the formability of titanium sheets. We examined the springback behavior of CP2 titanium sheets, which hot formed at elevated temperatures. The Grade 2 titanium sheets were formed using a U-shaped die and then scanned with a 3D scanner to measure springback behavior. Tensile test, Vickers hardness test, and microstructural analysis were carried out using specimens cut from the sidewall and bottom of the U-shaped profile to examine the effect of formability.

## 2. Experimental Methods

The chemical compositions and mechanical properties of CP2 titanium with a thickness of 1 mm were given in Table 1 and Table 2, respectively.

**Table 1.** Chemical compositions of CP2 titanium (wt%).

Material	C	O	N	H	Fe	Al	Ti
CP2 titanium	0.021	0.140	0.210	0.008	0.049	0.161	Balance

**Table 2.** Mechanical properties of CP2 titanium at room temperature.

Material	Tensile Strength (MPa)	Yield Strength (MPa)	Young's Modulus (GPa)	Elongation (%)	Hardness (HV)
CP2 titanium	344	280	105	20	140

In the sample preparation process, CP2 titanium sheets were cut into blanks with a size of 500×400 mm, and the blanks' length direction was along the rolling direction. The heating of the blanks was performed for 10 minutes in a conventional furnace for 350 °C, 450 °C, 550 °C, 650 °C, 750 °C, 850 °C and 950 °C. At the end of this process, the heated blanks were directly transferred to the press and subsequently formed. The transfer time from the furnace to the cold die was 5 s, and the temperature drop was around 50 °C.

The hot forming process was carried out on a 200 tons hydraulic press with 10 mm/s punch speed. The blanks were formed and held for 1 min between the die and punch. The experimental set-up and geometries of die and punch are shown in Fig. 1, in which the punch and die were made by tool steel.

The images of the U-profiles were taken with an Olympus digital camera with a white light scanning system to determine the springback behavior. A wireframe model was generated from the digital images, and texture mapping was done using the RapidForm software. The scanned data was registered into the CAD data to display the data sets by using the software. The springback behavior of the U-profiles was defined by the sidewall angle, having the most critical effect on dimensional accuracy and thus affects the subsequent assemblies [20]. The springback amount was measured by the angle ( $\theta$ ) between the deformed shape of the blank before and after springback (Fig. 2).

The tensile and hardness tests were performed to observe the mechanical properties of the U-profile CP2 titanium alloy. All tests were performed at room temperature. The specimens were cut from the vertical direction of the bottom and side-wall of the U-profile by using a laser-beam cutting machine, as shown in Figure 3 (a). The dimensions of specimens according to the ASTM E8 standards were given in Figure 3 (b). Tensile tests were performed at 10 mm/min constant strain rate on UTEST 25 tons universal tensile testing machine. The Vickers hardness test was applied using an indentation load of 0,5 kg and dwell time of 10 s, with Metkon Duroline-M hardness test machine. The hardness was measured from 5 different sample points for each sample and the average hardness values were calculated.

Microstructural analyses were performed using an optical microscope (Nikon MA100) at 50x, 100x, and 200x of magnification levels. For observing microstructure, the specimens were polished and etched with an etchant including 2% hydrofluoric acid (HF), 8% nitric acid (HNO<sub>3</sub>) and 90% pure water (H<sub>2</sub>O) for 20 s.

## 3. Results And Discussion

### 3.1. Mechanical Properties

Side-wall and bottom specimens of U-profile sheets formed at room temperature (RT), 350 °C, 450 °C, 550 °C, 650 °C, 750 °C, 850 °C and 950 °C were subjected to tensile test at room temperature, and results were plotted in Figure 4. It was observed that the strength and strain were mostly affected from elevated temperatures. The bottom specimens' strength had higher values on average, around 5-10% at all forming temperatures than sidewall specimens, except RT specimens. It is thought that this difference is because the bottom surface of the punch contacts the sheet earlier than the sidewall surfaces of the sheet during hot forming. So rapid cooling starts from higher temperatures of the bottom surface. Besides,

deformation hardening occurs due to compression by punch and die increase at the bottom surface of the blank.

The tensile strengths of the bottom specimens were slightly increased with increasing forming temperature until 850°C. There was obtained a considerable increase in strain and a decrease in tensile strength at 650 °C. After 850 °C, the strength increased dramatically, about 47% until 950 °C. When the true stress-true strain curves of specimens given in Figures 5a and 5b are examined, it is seen that significant strain hardening is observed at bottom specimens compared with sidewall samples. The true stress curve of the sidewall specimens became flat due to the ductile behavior of the material, indicating that the deformation rate is lower than the bottom region. Fig. 4 also shows the total strain results of the specimens. The total strain of the sidewall specimens was significantly higher than bottom specimens with increasing temperature, indicating that the deformation mechanisms vary with the deformation temperature and position of the sheet in the die. The sidewall specimens strain had higher values on average, around 15-33% at all forming temperatures than sidewall specimens, except for specimens formed at RT and 950°C. While a significant increase in strain has not occurred in bottom and sidewall specimens until 850 °C, it has decreased substantially between 850-950 °C. This decrease was about 65% for the sidewall specimens and about 50% for the bottom specimens, indicating that the micro constituents and microstructures varied with forming temperature.

The microhardness change of bottom and side-wall specimens of CP2 titanium hot formed at RT, 350°C, 450 °C, 550 °C, 650 °C, 750 °C, 850 °C and 950 °C is presented in Fig. 6. The hardnesses of bottom specimens were measured as higher than sidewall specimens. The increase was highest at 950 °C with 2%. Temperature-dependent hardness variation was obtained in both side-wall and bottom samples parallel to each other. This showed that the bottom surface specimens had a deformation hardening and rapid cooling effect.

### **3.2. Microstructures**

The microstructure evaluation of the formed sheets was given in Fig. 7. The microstructure images of bottom and sidewall samples are very similar, and consist of equiaxed grains except specimens hot formed at 850 °C. The sheets formed at room temperature consisted of equiaxed grains exhibiting the same twin bands, and the average diameter of the  $\alpha$  phase was in the size of 60-100  $\mu\text{m}$  (Fig. 7a and Fig. 7b). There are numerous carbides, mostly inside grains. It is seen that the microstructure does not change at 350 °C forming temperature at bottom and sidewall samples. Nevertheless, the few recrystallized grains occurrence was observed locally at 450 °C forming temperature at bottom samples. The start of recrystallization in sidewall samples was observed at higher temperatures (550 °C). However, recrystallization is more evident in the bottom wall. This was due to higher deformation rates and higher dislocation density for the bottom wall. Recrystallized grains are uniformly fine (with a diameter of around 20  $\mu\text{m}$ ) and equiaxed at these forming temperatures. In addition, twin intersections are seen where the dislocation density is high and the recrystallized grains are fine.

After this temperature, it is seen that the microstructure does not change until 750 °C forming temperature (Fig. 7b, Fig. 7c, Fig. 8b and Fig. 8c). But the number of twins was gradually decreased. Alpha grains were similar to room temperature-formed sheets with an average grain size of 80  $\mu\text{m}$ . At 750 °C, a slightly grain coarsening was seen with grain size 105  $\mu\text{m}$ . The grain size continued to increase at 850 °C. The position and quantity of the carbides were changed and became prominent. Heating above 850 °C caused a noticeable increase in the alpha grain size. Hot forming at 950 °C showed colonies of serrated bright etching  $\alpha$  plates and particles of dark etching retained  $\beta$ .

According to the literature [23], beta particles are formed at high temperatures (between 900-950 °C). Because this temperature is the beta transus temperature which alpha grains transform to beta grains, but on the other hand, the presence of acicular alpha is also seen at this temperature.

### 3.3. Fracture Morphology

In this study, the fracture surfaces of the tensile samples cut from the formed materials at room temperature, 350, 750, 850 and 950 °C were investigated. According to the bottom specimens, dimples are seen at room temperature and 350 °C, representing ductile fracture. At 350 °C, an increase in the number of dimples was observed, and there is elongation in the dimples. Therefore, higher ductility is expected at 350 °C, and according to Figure 8, a higher strain value occurred at 350 °C. There are dimples and voids at 750 °C. In some areas, dimples have become smaller. Voids and small dimples are known to reduce ductility. Indeed, the total strain has dropped at 750 °C in Figure 8. At 850 °C, it is seen that voids are in a state of disappearance. For this reason, the total strain and ductility slightly increased. There are smooth and shiny surfaces at 950 °C, representing brittle failure, and the lowest strain value was also obtained at this temperature. When the temperature increased from room temperature to 350 °C, the dimples were elongated in some regions and the dimples have also increased. This indicates an increase in ductility and Figure 9 supports this. Micro voids are available at 750 °C and have an effect reduces ductility. At 850 °C, dimples became smaller and the ductility decreases. Brittle fractures are observed, and therefore, smooth and shiny surfaces are formed at 950 °C. Because of this reason, the lowest strain value was obtained at 950 °C. The brittle fracture causes low ductility.

Besides, when the macroscopic photographs of the samples given in Figure 10 are examined, ductile fracture type is seen in all samples except the sample at 950 °C.

### 3.4. Springback Angles

The temperature up to room temperature is found to be effective for reducing the strength. However, the decrease in strength does not mean an increase in formability in this temperature range. The formability results are seen in Table 3. According to the figure, it increased after 350 °C. As known from the literature, Ti has a hexagonal close-packed (HCP) crystal structure with a limited number of slip planes. For this reason, Ti has lower formability at RT, but at high temperatures, the existence of alternative slip systems improves the formability [13]. The findings at high temperatures have supported the mentioned reason.

Springback is commonly related to high strength and elastic energy. As the temperature is increased, the strength of the material is also substantially increased, and the high strength of a sheet material indicates the greater the degree of springback.

**Table 3.** Springback angles of hot formed sheets.

Temperature	RT	350	450	550	650	750	850	950
Angle (°)	15	12	10	8	9	9	10	11

## 4. Conclusion

In this paper, the formability properties of Grade 2 titanium sheets were examined. The materials were heat-treated and bent with a U-shaped die. After the bending process, springback angles were measured. To observing the effects of mechanical and microstructural properties on springback behavior, tensile test, hardness test, and microstructural analysis were carried out. The main results are as follows:

The bottom specimens' strength and hardness had higher values than sidewall specimens, because rapid cooling starts earlier on the bottom surface, and deformation hardening is observed. Side strain values were obtained higher than bottom strain values. This showed that the position of the sheet in the mold affected the mechanical properties. The highest strength value and the lowest strain value were obtained at 950 °C in all samples. The high springback value obtained at room temperature was reduced by forming at high temperatures. Thus, when the forming process at high temperatures is selected as an alternative, it provides both higher strength and a lower springback than room temperature.

## Declarations

**Funding** This research is part of a project supported by The Commission of Scientific Research Projects of Bursa Uludag University (Project No: OUAP(MH)-2015/11).

**Conflicts of interest/Competing interests** The authors declare no competing interests.

**Availability of data and material** The authors confirm that the data supporting the findings of this study are available within the article.

**Code availability** Not applicable

## Acknowledgments

This work is part of a project supported by The Commission of Scientific Research Projects of Bursa Uludag University (Project No: OUAP(MH)-2015/11). The authors would like to thank the department for the valuable support.

## Data availability statement

The data used to support the findings of this study are available from the corresponding author upon request.

## References

1. Polmear MQI, StJohn D, Nie JF (2017) *Light Alloys: Metallurgy of the Light Metals*, 5th edn. Elsevier
2. Leyens C, Peters M (2003) *Titanium and titanium alloys: fundamentals and applications*. John Wiley & Sons
3. Boyer RR (1996) An overview on the use of titanium in the aerospace industry. *Materials Science Engineering: A* 213:103–114. [https://doi.org/10.1016/0921-5093\(96\)10233-1](https://doi.org/10.1016/0921-5093(96)10233-1)
4. Gupta RK, Kumar VA, Xavier XR (2018) Mechanical Behavior of Commercially Pure Titanium Weldments at Lower Temperatures. *J Mater Eng Perform* 27:2192–2204. <https://doi.org/10.1007/s11665-018-3307-9>
5. Boyer R, Gerhard W, Collings EW (1994) *Materials Properties Handbook: Titanium Alloys*. ASM International, Materials Park
6. Ahmed YM, Sahari KSM, Ishak M, Khidhir BA (2014) Titanium and its alloy. *International Journal of Science Research* 3:1351–1361
7. Donachie MJ (1988) *Titanium - A technical guide*. ASM Int. Met, Park. OH 44073
8. Kikuchi S, Akebono H, Ueno A, Ameyama K (2018) Formation of commercially pure titanium with a bimodal nitrogen diffusion phase using plasma nitriding and spark plasma sintering. *Powder Technol* 330:349–356. <https://doi.org/10.1016/j.powtec.2018.02.047>
9. Beal JD, Boyer R, Sanders D (2006) Forming of Titanium and Titanium Alloys. *ASM Hand B* 14:656–669. <https://doi.org/10.31399/asm.hb.v14b.a0005146>
10. Rahmani B, Alinejad G, Bakhshi-Jooybari M, Gorji A (2009) An investigation on springback/negative springback phenomena using finite element method and experimental approach. *Proceedings of the Institution of Mechanical Engineers: Part B* 223:841–850. <https://doi.org/10.1243/09544054JEM1321>
11. Tekiner Z (2004) An experimental study on the examination of springback of sheet metals with several thicknesses and properties in bending dies. *J Mater Process Technol* 145:109–117. <https://doi.org/10.1016/j.jmatprotec.2003.07.005>
12. Ozturk F, Ece RE, Polat N, Koksall A (2010) Effect of warm temperature on springback compensation of titanium sheet. *Mater Manuf Processes* 25:1021–1024. <https://doi.org/10.1080/10426914.2010.492056>
13. Gisario A, Barletta M, Venettacci S (2016) Improvements in springback control by external force laser-assisted sheet bending of titanium and aluminum alloys. *Opt Laser Technol* 86:46–53. <https://doi.org/10.1016/j.optlastec.2016.06.013>

14. Zhao Y, Peng L, Lai X (2018) Influence of the electric pulse on springback during stretch U-bending of Ti6Al4V titanium alloy sheets. *J Mater Process Technol* 261:12–23. <https://doi.org/10.1016/j.jmatprotec.2018.05.030>
15. Hamedon Z, Mori K, Maeno T (2013) Hot stamping of titanium alloy sheet using resistance heating. *Vestnik of Nosov Magnitogorsk State Technical University* 5:12–15
16. Khayatzadeh S, Thomas MJ, Millet Y, Rahimi S (2018) Characterisation and modelling of in-plane springback in a commercially pure titanium (CP-Ti). *Journal of Materials Science* 53:6872–6892. <https://doi.org/10.1007/s10853-017-1983-8>
17. Li H, Yang H, Song FF, Zhan M, Li GJ (2012) Springback characterization and behaviors of high-strength Ti-3Al-2.5V tube in cold rotary draw bending. *J Mater Process Technol* 212:1973–1987. <https://doi.org/10.1016/j.jmatprotec.2012.04.022>
18. Badr OM, Rolfe B, Zhang P, Weiss M (2017) Applying a new constitutive model to analyze the springback behaviour of titanium in bending and roll forming. *Int J Mech Sci* 128–129:389–400. <https://doi.org/10.1016/j.ijmecsci.2017.05.025>
19. Ao D, Chu X, Yang Y, Lin S, Gao J (2018) Effect of electropulsing on springback during V-bending of Ti-6Al-4V titanium alloy sheet. *The International Journal of Advanced Manufacturing Technology* 96:3197–3207. <https://doi.org/10.1007/s00170-018-1654-1>
20. Gheysarian A, Abbasi M (2017) The Effect of Aging on Microstructure, Formability and Springback of Ti-6Al-4V Titanium Alloy. *J Mater Eng Perform* 26:374–382. <https://doi.org/10.1007/s11665-016-2431-7>
21. Niu L, Wang S, Chen C, Qian SF, Lie R, Li H, Liao B, Zhong ZH, Lu P, Wang MP, Li P, Wu YC, Cao LF (2017) Mechanical behavior and deformation mechanism of commercial pure titanium foils. *Materials Science Engineering: A* 707:435–442. <https://doi.org/10.1016/j.msea.2017.09.080>
22. Titanium Grade 2 (2018) Available: <http://asm.matweb.com>. [Accessed: 26-Sep-2018]
23. Akyazi T (2011) Investigation of surface properties of plasma nitrided and PVD coated Ti- 6Al-4V alloy for biomedical applications, Master's thesis, Istanbul Technical University, Istanbul

## Figures

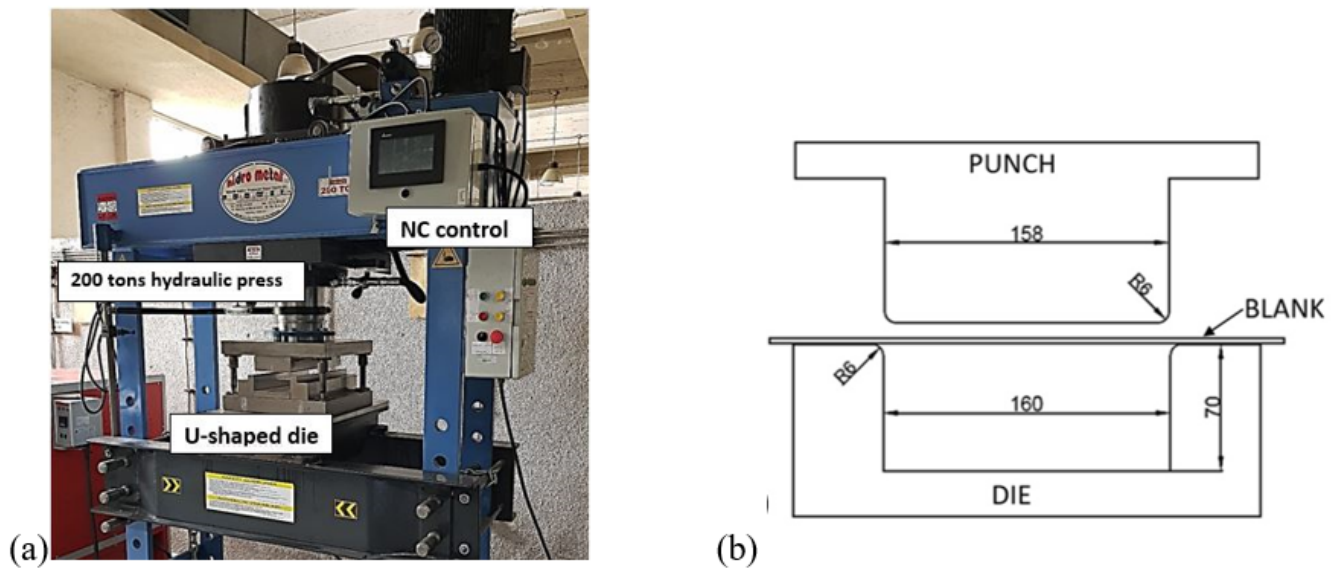


Figure 1

The experimental set-up of (a) hydraulic press and (b) geometries of die and punch used for hot forming.

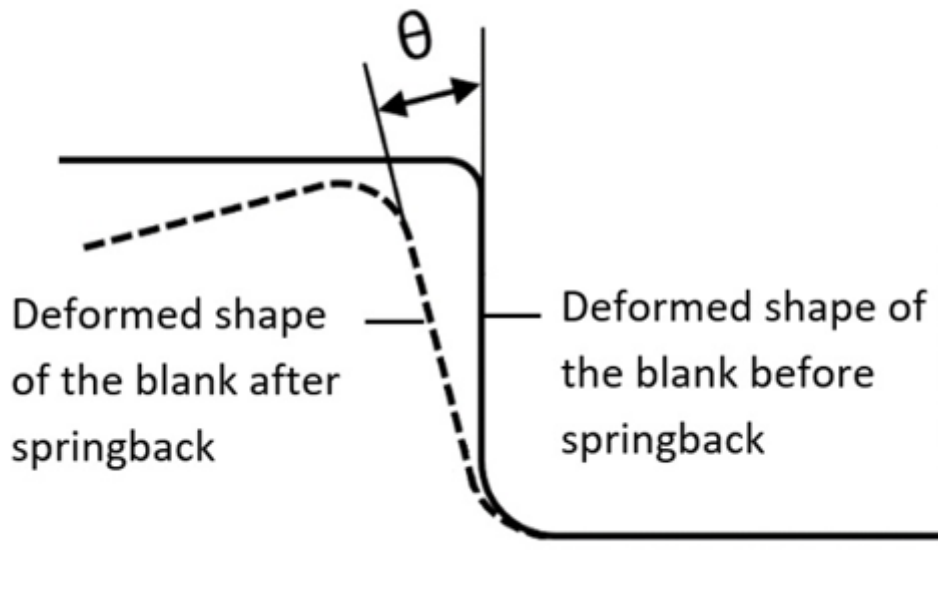
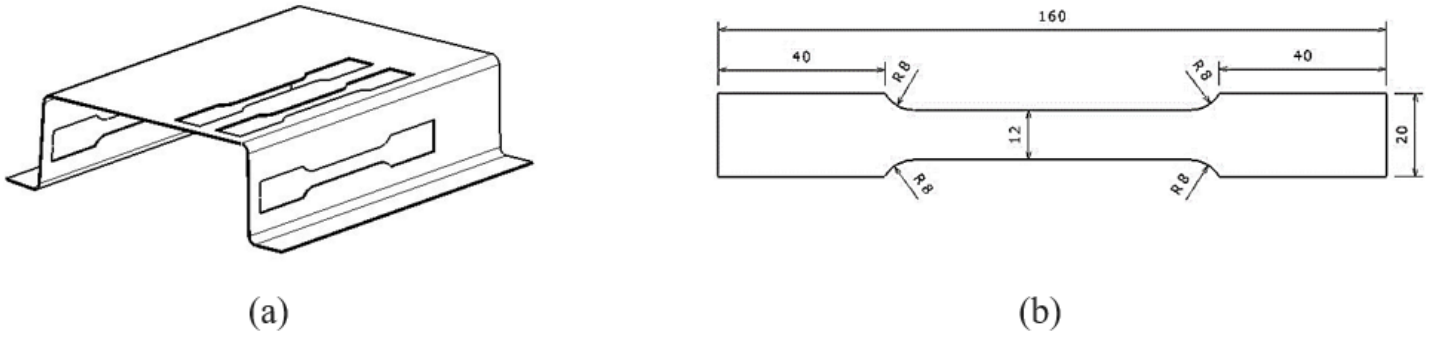


Figure 2

Schematic representation of the springback angle in the U-profile.



**Figure 3**

(a) Cutting areas of the samples on the U-shaped profile and (b) tensile specimens dimensions in mm.

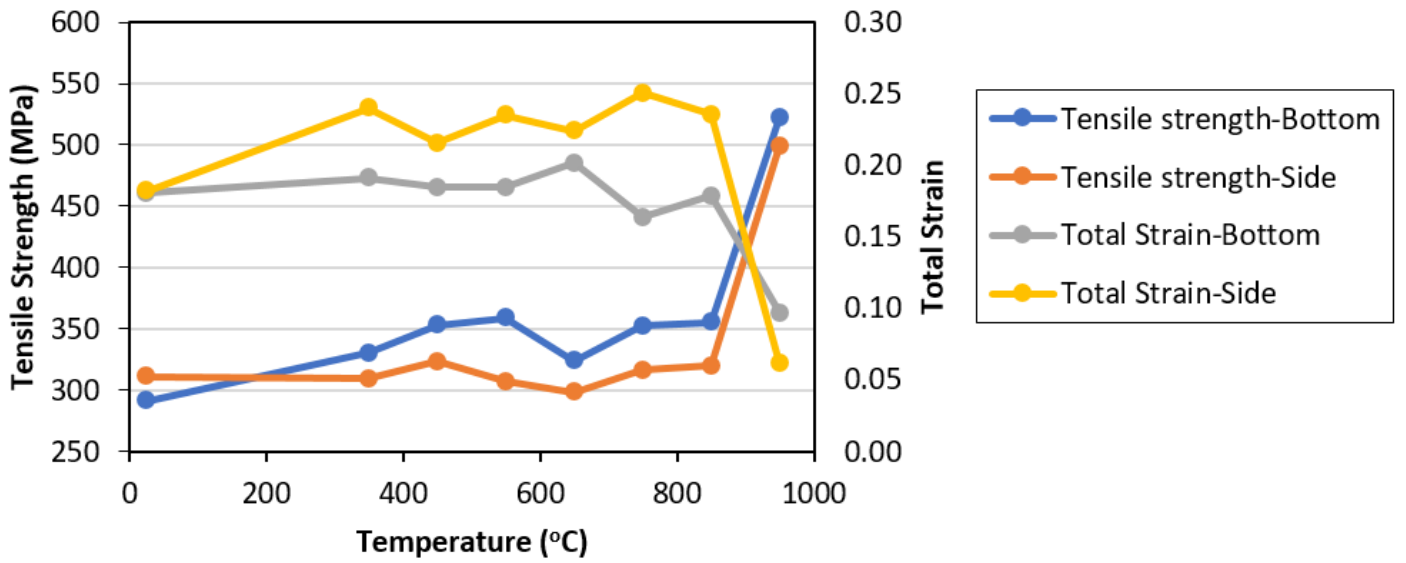
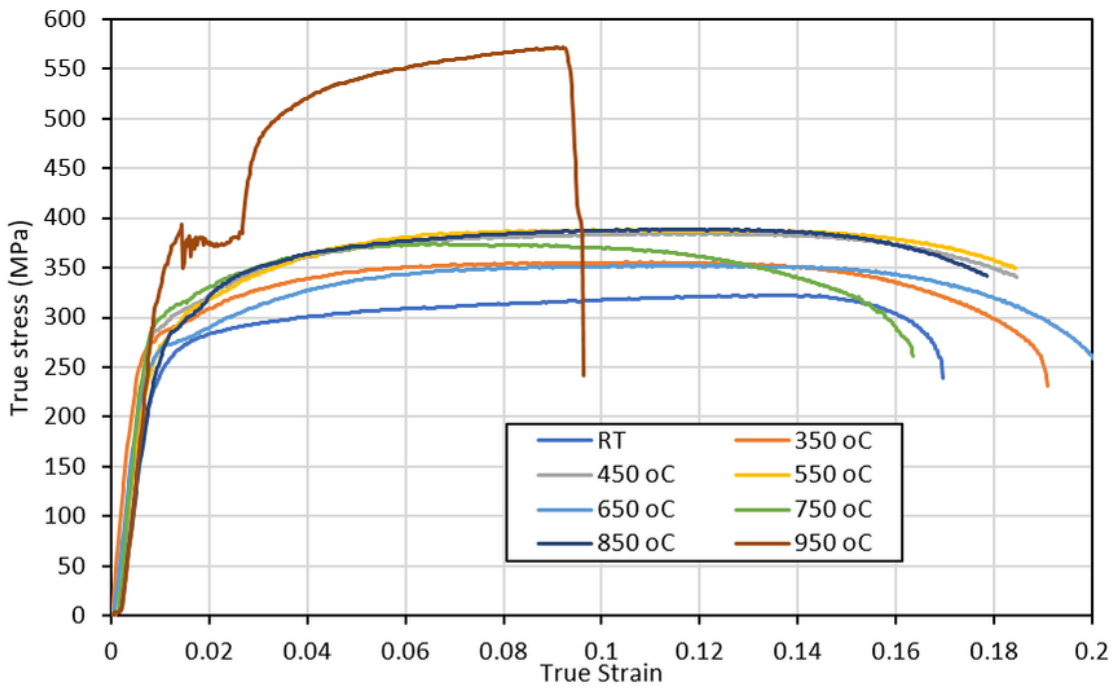
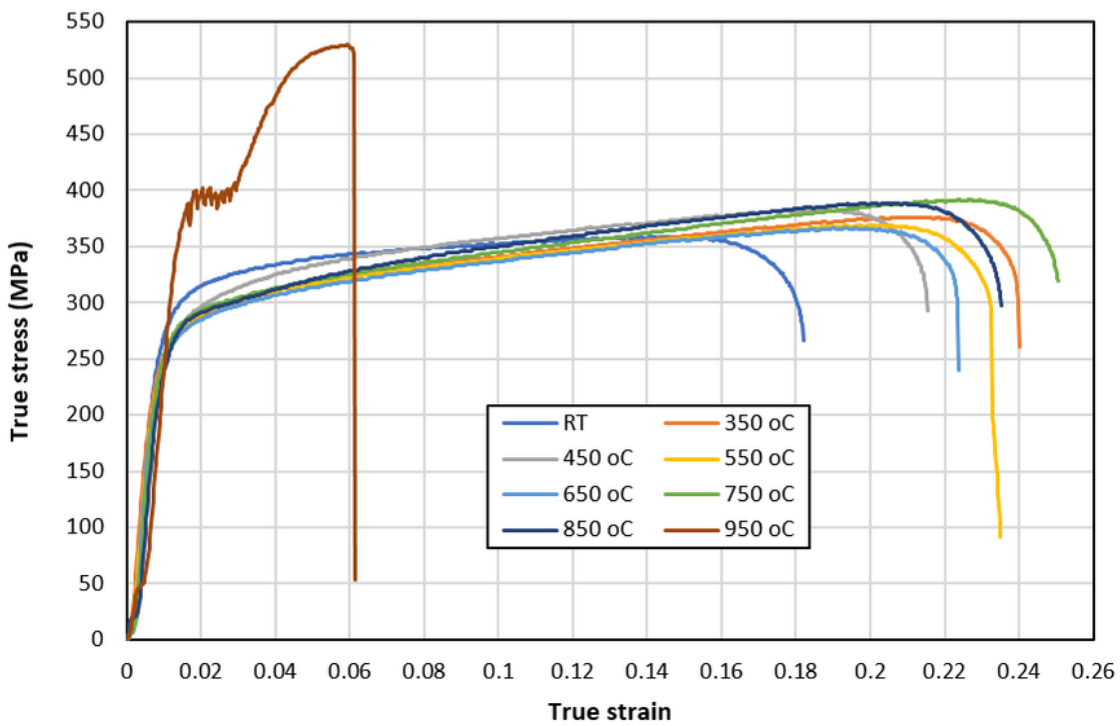


**Figure 4**

The effect of the temperature on tensile strength and total strain



(a)



(b)

**Figure 5**

Stress-strain curves of samples taken from (a) boottom and (b) side-wall of CP2 titanium blanks hot formed in various temperatures.

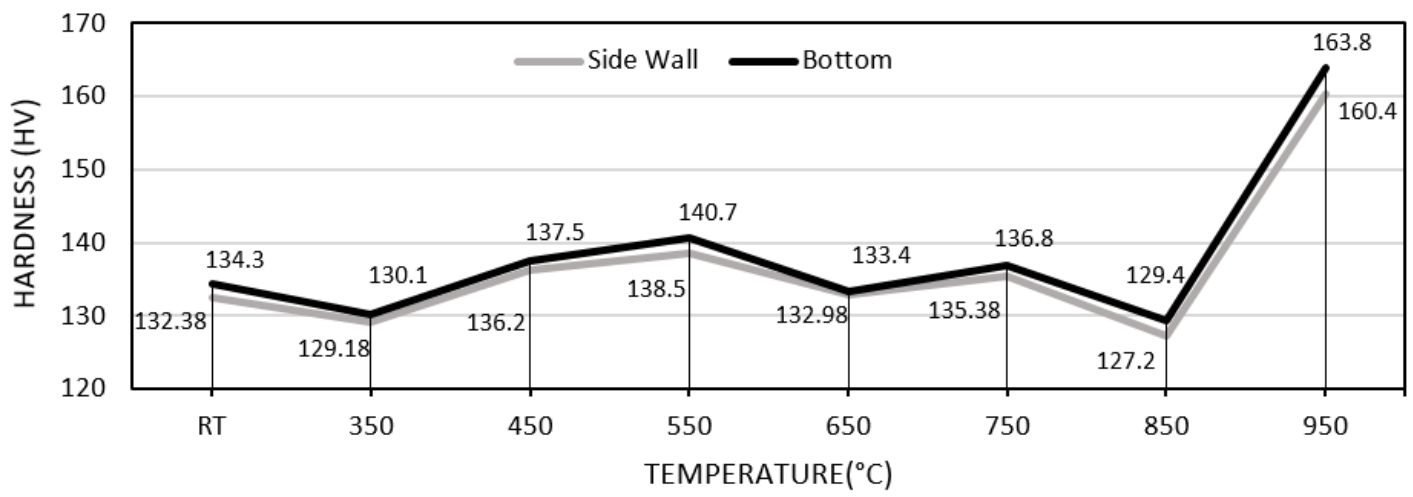


**Figure 6**

Microhardness change of CP 2 titanium sheets hot formed in various temperatures

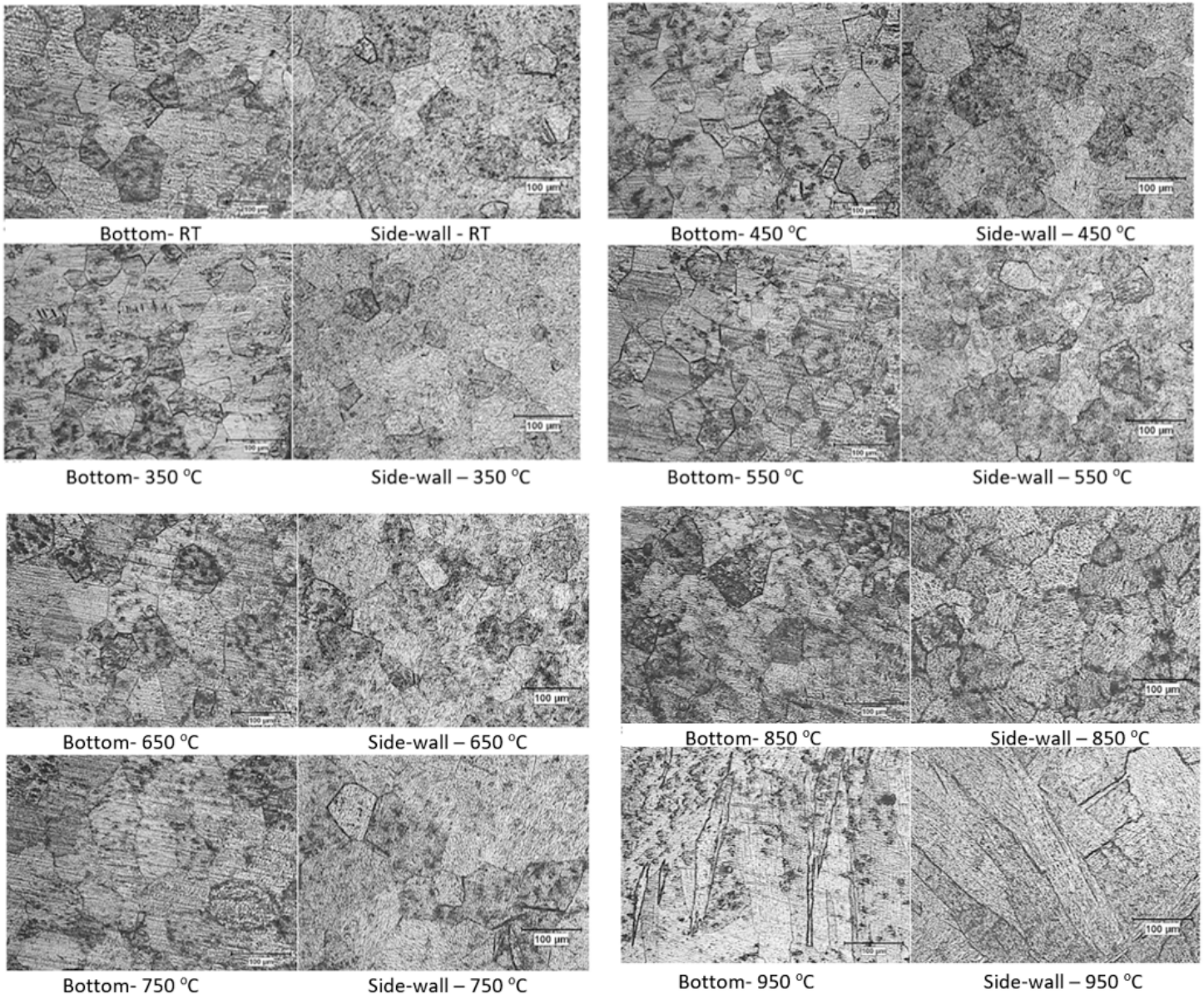


**Figure 7**

Microstructure characteristics of commercially pure titanium Grade 2 sheets at different temperatures.

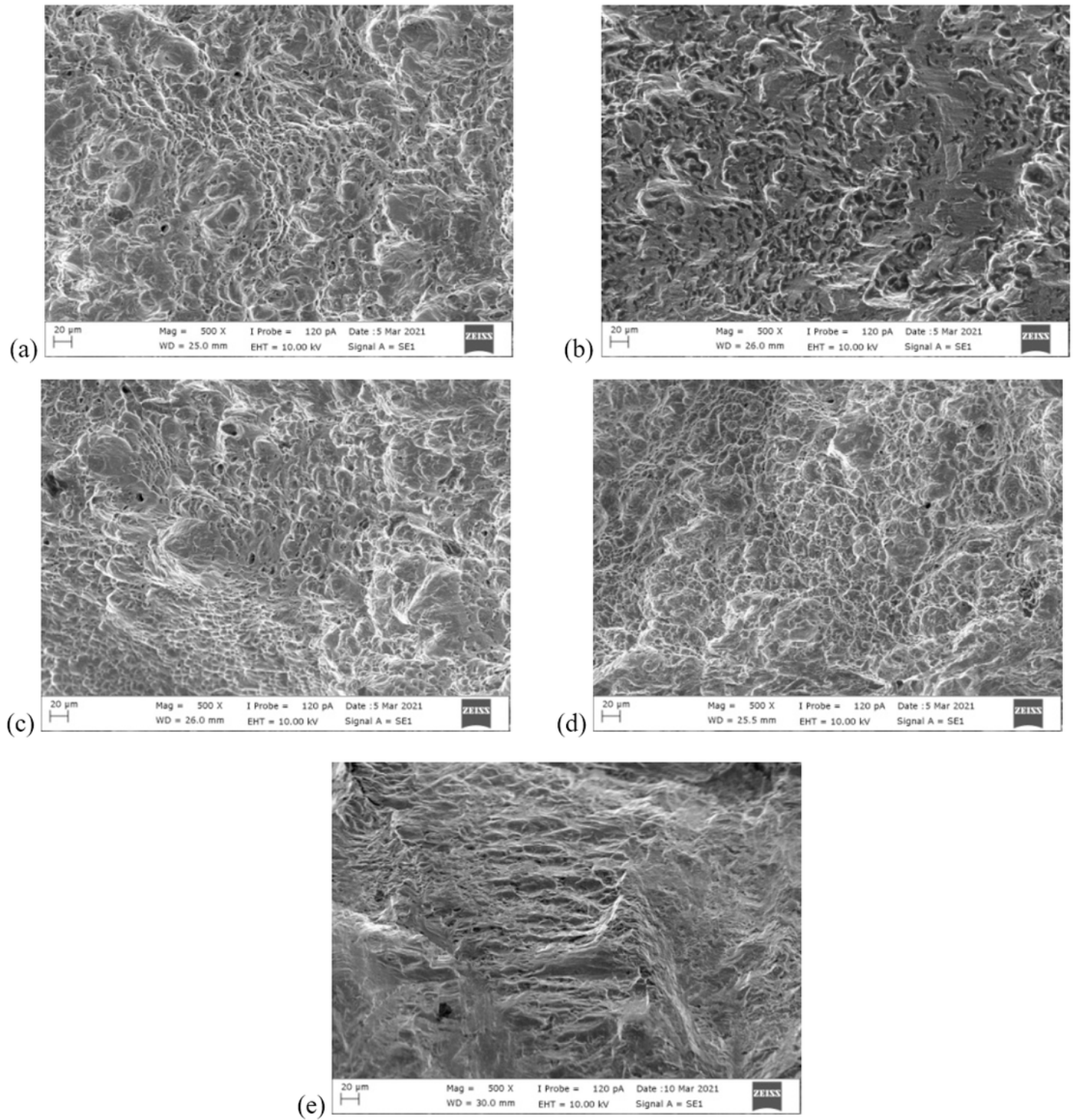


**Figure 8**

Fracture morphology of the specimens taken from bottom side of the U profile hot formed in (a) RT, (b) 350 °C, (c) 750 °C, (d) 850 °C and (e) 950 °C.

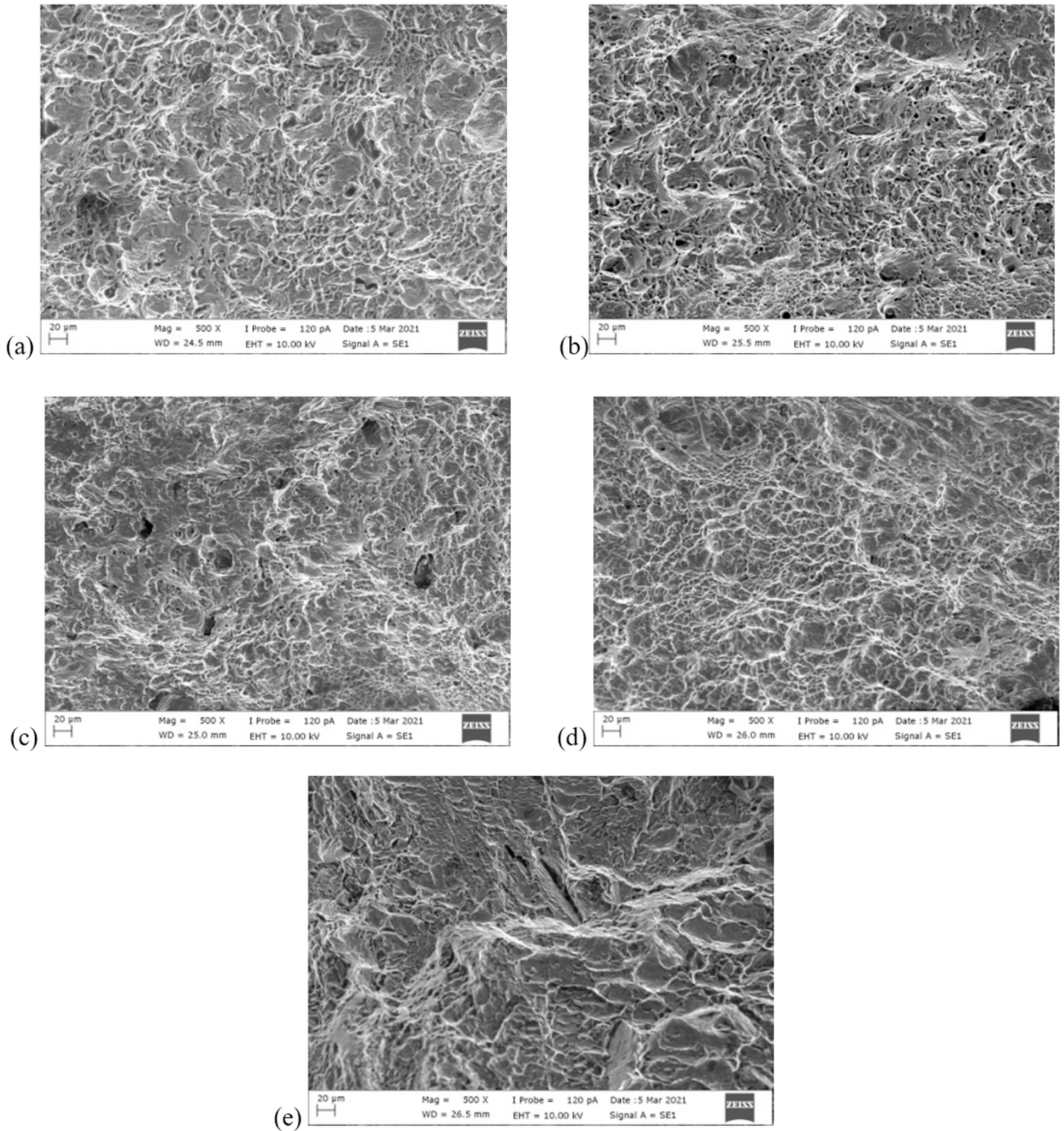


**Figure 9**

Fracture morphology of the specimens taken from side-wall of the U profile hot formed in (a) RT, (b) 350 °C, (c) 750 °C, (d) 850 °C and (e) 950 °C.

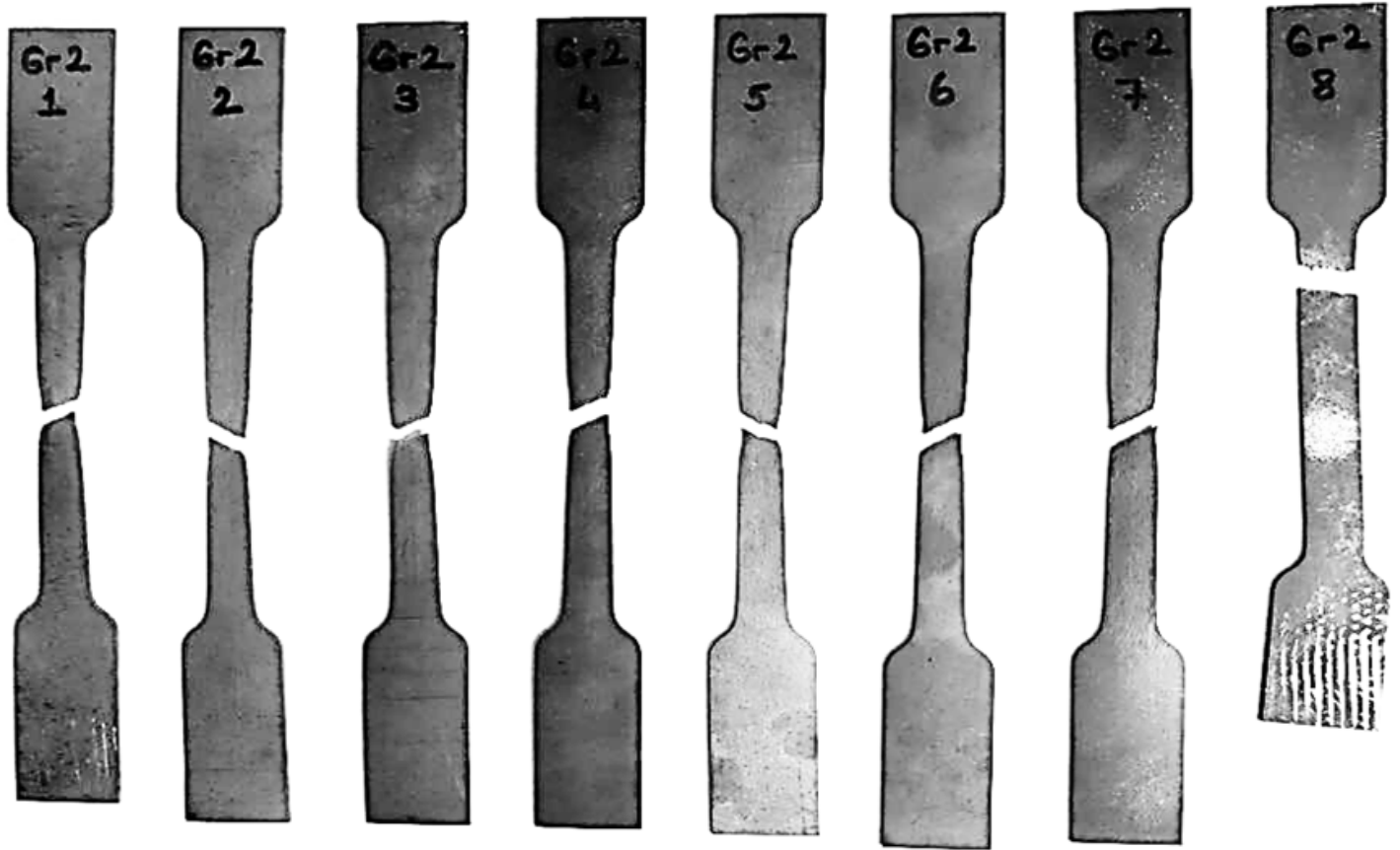


Figure 10

Macroscopic images of fractured samples.